^{125}I-Labeled Gold Nanorods for Targeted Imaging of Inflammation

Xia Shao,[†] Huanan Zhang,[‡] Justin R. Rajian,[†] David L. Chamberland,[§] Phillip S. Sherman,[†] Carole A. Quesada,[†] Alisa E. Koch,[§] Nicholas A. Kotov,[‡] and Xueding Wang[†,*]

[†]Department of Radiology, [‡]Department of Chemical Engineering, and [§]Department of Internal Medicine, University of Michigan, Ann Arbor, Michigan 48109, United States

ABSTRACT

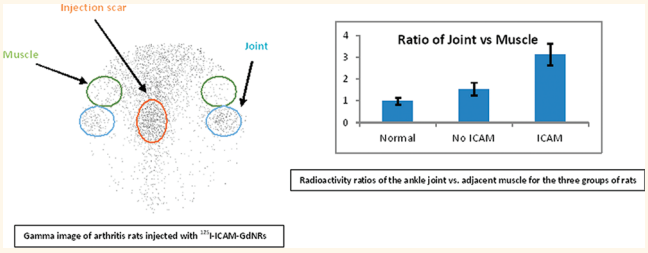

For better examination of inflammation, we designed inflammation-targeted nuclear and optical dual-modality contrast agents prepared by I-125 radiolabeling of gold nanorods (GdNRs) conjugated with anti-intercellular adhesion molecule 1 (ICAM-1) antibody. The bioactivity and specific binding of the PEGylated ^{125}I-ICAM-GdNR conjugates to the ICAM-1 was validated through ELISA testing. Inflammation-targeted imaging was then conducted on an adjuvant-induced arthritic rat model which demonstrated an elevation of ICAM-1 level in the affected ankle joints. Facilitated by the I-125 radioisotope and the whole-body imaging *via* the Gamma camera, the time-dependent distribution of the systemically injected agent as well as the uptake of the agent in the inflammatory articular tissues could be examined conveniently and quantitatively. The success in targeted delivery of gold nanoparticles to inflammatory tissue enables both nuclear and optical imaging of inflammation at molecular or cellular level. Other than diagnosis, radiolabeled gold nanoparticles also hold promise for targeted therapy of a variety of disorders.

KEYWORDS: gold nanorods · iodine-125 · γ-imaging · radiolabeled nanoparticles · inflammation

Rheumatoid arthritis (RA) is a chronic systemic inflammatory disorder of unknown etiology which produces a persistent inflammation of the synovial membrane.[1] Although RA is serious, potentially crippling, and commonly disabling, comprehensive diagnosis and optimized therapies of these disorders are hindered by lack of technologies that can image inflammation at molecular or cellular level.[2] Several studies have demonstrated that an imbalance occurs in the cytokine cascade resulting in the presence of pro-inflammatory cytokines in synovium and plasma, which leads to the joint inflammation and cartilage destruction characteristic of RA. Attention has therefore been given to develop inhibitors of pro-inflammatory cytokines and their receptors. Monoclonal antibodies (mAbs) specifically target pro-inflammatory cytokines and membrane-bound receptors and thereby interfere with specific inflammation pathways at the molecular level.[3,4] These mAbs have been used for treatment of RA patients and also been radiolabeled for molecular imaging of RA.[5] As an example, a pretherapy scintigraphic approach with radiolabeled mAbs may allow evaluation of the presence of target molecules in the inflammatory lesion, thus aiding the selection of the most efficient therapy.[6] Development of new probes and new technologies for targeted imaging and *in vivo* evaluation of pro-inflammatory cytokines and membrane-bound receptors may significantly contribute not only to clarify the pathophysiology of different inflammatory diseases but also to improve the detection of pathological changes at the molecular level in a very early stage.

Recently, the development of gold nanoparticles (GdNPs) as contrast agents for medical imaging and vehicles for drug delivery have undergone a dramatic expansion. GdNPs are ideal optical labeling materials due to their unique optical properties as well as their good biocompatibility, stability, and ease of preparation and bioconjugation.[7−9] In former studies, a variety of GdNPs including gold nanorods (GdNRs), gold nanocages, and gold nanoshells have been introduced as targeting or nontargeting contrast agents for photoacoustic imaging (PAI), an emerging optical imaging technology which is also referred to as optoacoustic imaging.[10−13] As a novel strategy for drug delivery, GdNPs can potentially enlarge the carrier capacity and enable controlled drug release, minimizing the toxicity and enhancing the therapeutic

* Address correspondence to xdwang@umich.edu.

Received for review August 16, 2011 and accepted October 17, 2011.

Published online October 17, 2011
10.1021/nn203138t

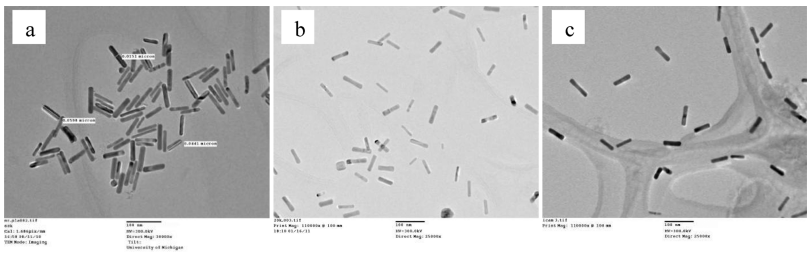

Figure 1. TEM images of bare GdNRs (a), conjugates of GdNRs with ICAM-1 antibody (b), ICAM-GdNRs radiolabeled with ^{125}I (c).

efficiency.[14−16] The surface chemistry of GdNPs allows multiple functionalizations. Capping molecules, such as cetyltrimethylammonium bromide (CTAB), can be replaced or conjugated with many functional groups.[17−19] Target specificity of GdNPs can be imparted by tagging with certain biovectors, such as monoclonal antibodies,[20] receptor-specific peptides,[8] and other compounds.[7,21] However, many questions still need to be addressed before GdNPs could be widely adapted in clinical settings. For example, how the size, shape, material, and surface chemistry is going to affect their optical property, toxicity, molecular response, carrier capacity, and ability to arrive at the targeted tissues. Moreover, how do GdNPs perform in the complex *in vivo* environments of human or animals where a variety of ions, such as hydrogen, Na, Cl, and Ca, as well as proteins, lipids, and hydrocarbons, may strongly affect their stability and functionality. Without an imaging technology that could monitor the *in vivo* behavior of GdNPs, systemic evaluation and optimization of GdNPs as imaging and therapeutic agents is challenging.

In our previous work, by radiolabeling GdNRs with I-125, a dual-modality contrast agent has been fabricated which can be imaged *in vivo* with both PAI and nuclear imaging.[22] With high sensitivity, nuclear imaging enables whole-body quantification evaluation of radiolabeled GdNRs and, hence, can be used for systemic evaluation of novel GdNP agents *in vivo*.[23] Although with comparatively lower sensitivity, PAI could present tissue structures with spatial resolution on the submillimeter level and, therefore, can be superior in mapping the distribution of GdNPs in regional target tissues. By fabricating the radiolabeled GdNPs performing dual-modality imaging, one may combine the high contrast-to-noise ratio and good quantification of nuclear imaging with the high spatial resolution of PAI. In this study, we explored the feasibility of targeted delivery of GdNRs to inflammatory tissues by conjugating with intercellular adhesion molecule 1 (ICAM-1) antibody, a pro-inflammatory cytokine, uptakes of GdNRs in the inflammatory joints of bacterial induced arthritic rats. Using the radiolabeling method recently developed in our group, quantification of ICAM-1 expression in arthritic joints was attempted.

RESULTS AND DISCUSSION

Radiolabeling of GdNR Conjugates with Anti-ICAM-1. GdNRs with average aspect ratios of 4 were obtained with transverse plasmon peak at 525 nm and longitudinal plasmon peak at around 800 nm. The position of the longitudinal plasmon peak could be fine-tuned fairly easily within 600−900 nm ranges by varying the content of silver nitrate during synthesis. The shape and size of GdNRs remains unchanged before and after conjugation based on the transmission electron microscopy (TEM) images shown in Figure 1.

The radiolabeling reaction takes place very rapidly and completely with radiochemical yields greater than 90% by radioactivity count and specific activity greater than 5×10^5 Ci/mmol. There was no apparent difference between bare GdNR and ^{125}I-ICAM-PEG-GdNRs (Figure 1). The longitudinal plasmon peaks remain unchanged in intensity after radiolabeling but show a small plasmon shift due to the presence of additional iodine molecules on the surface.[23] [^{125}I]-Iodine-labeled GdNRs were stable for weeks when stored in the refrigerator.[23] This simple radiolabeling procedure facilitates reproducibility and reliability of the injected product for animal studies. This simple setup could be extensively utilized to deliver injectable doses for clinical application, with the availability of our well-equipped radiopharmaceutical laboratory.

Enzyme-Linked Immunosorbent Assay of ICAM-1 Antibody. ICAM-1 is a glycosylated protein of 80−114 kDa with a core polypeptide of 55 kDa and has an important role in leucocyte trafficking and cell−cell adherence in immunological responses.[24,25] ICAM-1 is induced during inflammatory responses by cytokines such as IL-1.[26] In RA, endothelial cells expressing ICAM-1 establish contact with circulating leucocytes, resulting in accumulation of leucocytes in synovial tissues of joints. Compared with the serum concentrations in osteoarthritis (OA) patients, the serum concentrations of soluble ICAM-1 are significantly higher in patients with RA and correlate with markers of disease activity such as the erythrocyte sedimentation rate and C-reactive protein levels.[27] Furthermore, anti-ICAM-1 monoclonal antibody therapy results in a transient alteration in T-lymphocyte recirculation and leads to clinical improvement in some RA patients.[28] Recent studies have also demonstrated that ICAM-1 signal is involved in

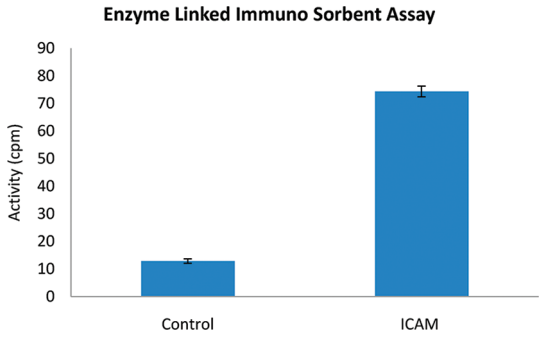

Figure 2. Mean and standard deviation of radioactivities of the ELISA wells treated, respectively, with radiolabeled bare GdNRs (control) and radiolabeled GdNRs conjugated with ICAM-1 antibody (ICAM).

Fas-mediated apoptosis in RA synovitis.[29] Due to important roles for ICAM-1 in the pathology of RA,[30] we choose ICAM-1 antibody as an inflammation-targeted imaging probe.

In addition, rapid clearance of nanoparticles from blood limits their targeting capabilities. Polyethylene glycol (PEG) has well-established "stealth" properties that can shield nanoparticles from fouling by serum proteins (opsonization) and reduce their rate of clearance by the reticuloendothelial system (RES) of the body.[7,18] The beneficiary effects of PEGylation on the clearance time of injected nanoparticles have been demonstrated.[20,31] Significant differences between bare GdNRs and PEGylated GdNRs have been observed from our previous experiments.[23] Injected bare GdNRs were cleared out from the blood circulation within 10 min, while more than 50% of PEG-coated GdNRs remained in the blood after 4 h. This is in good agreement with previous studies which have shown that a surface brush layer of PEG reduces the adsorption of blood RES factors to the particle surface, hence decreasing the rate of particle clearance. This gives GdNRs enough time to find their target. Therefore, PEGylated GdNRs have been used in all experiments. The long-term presence of the PEGylated GdNR agents in the circulatory system up to 4 h was monitored using a gamma camera.[23]

To determine the biological activity and specific binding of ^{125}I-ICAM-PEG-GdNRs, we performed an enzyme-linked immunosorbent assay (ELISA). The ELISA plate was coated by rat recombinant ICAM-1, and then radiolabeled PEGylated GdNR control and ICAM-1 antibody-conjugated GdNR solution were added to each corresponding well and incubated at room temperature for 2 h. The data are shown in Figure 2. In comparison with the wells that were added with radiolabeled bare GdNRs, the wells that were added with GdNRs conjugated with ICAM-1 antibody produced obviously stronger signals in the Gamma Imager. The activities were 74.3 $\pm$ 1.9 and 12.9 $\pm$ 0.8 in the wells containing radiolabeled ICAM-1 antibody-conjugated GdNRs and radiolabeled bare GdNRs, respectively. The ratio between radioactivities resulting from the specific and the nonspecific binding of radiolabeled GdNRs was 5:1. The ICAM-1 antibody conjugates showed five times higher affinity binding to ICAM-1 than the bare GdNRs. This finding from the ELISA experiment concludes that the ICAM-1 antibody conjugated with ^{125}I-labeled GdNRs retains its biological activity and forms a highly specific system.

Gamma Imaging of Arthritic Rats *in Vivo*. Encouraged by the positive ELISA findings, we then evaluated ^{125}I-ICAM-GdNRs *in vivo* with an arthritic rat model. Adjuvant-induced arthritis (AIA) rat, as one of the well-established rodent models for human inflammatory diseases similar clinically and pathologically to human RA, has been chosen for animal *in vivo* studies. The rats were injected subcutaneously into the base of the tail with lyophilized *Mycobacterium butyricum* to generate the adjuvant-induced arthritis. After 20 days, the ^{125}I-labeled GdNR agents were systemically injected *via* lateral tail veins. Imaging was conducted on three groups. Group A as a control was normal rats injected with targeting ^{125}I-ICAM-GdNRs agent. Group B as another control was arthritic rats injected with nontargeting ^{125}I-GdNRs agent. Group C was arthritic rats injected with targeting ^{125}I-ICAM-GdNRs agent. Figure 3 shows example images from the three groups (24 h post-injection). Although AIA is a systemic arthritis attacking all of the joints, the hind limb ankle joints of the AIA rats were the targets of imaging in this study because they were the most affected joints. Thus, animals were positioned ventral side down with the hind limbs placed in the middle of the field of view of the imager. Each image has a diameter of 8 cm covering the rear part of the rat body with the rat head pointing up. The biodistribution of ^{125}I-labeled GdNR agents, both PEGylated and non-PEGylated, has been studied in our previous work.[23] In this work, the imaging area covered only the rear part of the rat body focusing on the arthritic ankle joints.

Regions of interest (ROIs) were drawn respectively around each ankle joint and the adjacent muscle area as the control for each animal. The ratios between the radioactivities from the inflammatory ankle joint and the non-inflammatory muscle were calculated based on radioactive counts. The average and the standard deviation of each group were computed over the measurements from a total number of 10 ankle joints from the five rats. Figure 4 shows the quantitative analysis of the three groups.

As shown in Figure 4, the average ratios of the three groups were 0.98 $\pm$ 0.15, 1.53 $\pm$ 0.29, and 3.12 $\pm$ 0.48 for groups A, B, and C, respectively. The arthritic rats (group C) injected with ^{125}I-ICAM-GdNRs targeting inflammation had three times more uptake of the agent compared with the normal rats (group A) injected with the same agent. In comparison with nonspecific targeting (group B), the targeted delivery ^{125}I-ICAM-GdNRs

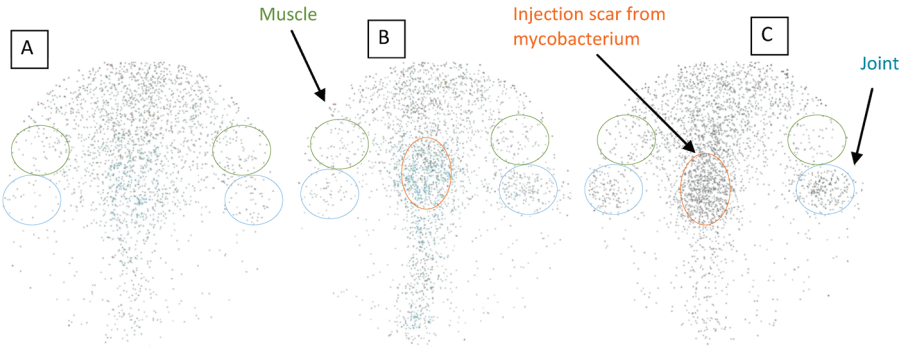

Figure 3. Inflammation-targeted nuclear and optical dual-modality contrast agent, prepared by I-125 radiolabeling of gold nanorods (GdNRs) conjugated with anti-intercellular adhesion molecule 1 (ICAM-1) antibody, acting as a biovector to navigate ^{125}I-labeled GdNRs to the arthritic joint.

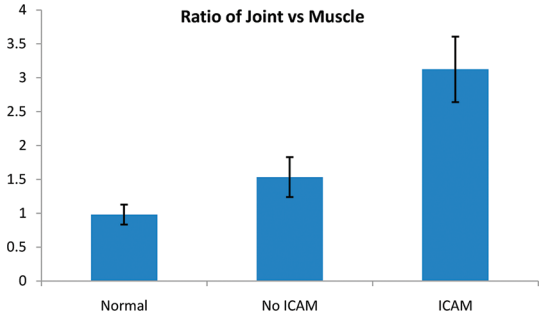

Figure 4. Radioactivity ratios of the ankle joint *vs* adjacent muscle for the three groups of rats, *i.e.*, normal rats injected with ^{125}I-ICAM-GdNRs (normal), arthritis rats injected with ^{125}I-GdNRs (no ICAM), and arthritis rats injected with ^{125}I-ICAM-GdNRs (ICAM).

(group C) based on the specific targeting of ICAM-1 led to a stronger (>2 times) regional uptake of the GdNRs. This agreed with reported findings that ICAM-1 was accumulated in the inflammatory articular tissues and also supported that ICAM-1 antibody acted as a biovector to navigate ^{125}I-labeled GdNRs to the arthritic joints. It should be noticed that there was enhanced radioactivity around the injection scars for all arthritic rats in both group B and group C because these areas had a greater inflammatory response after the injection of *Mycobacterium butyricum* (Figure 3). The arthritic rats injected with nontargeting ^{125}I-GdNRs agent (without ICAM-1 antibody) showed a slightly higher joint uptake than those of the normal rats. This is most likely due to leakage nature of the blood vessels in inflammatory articular tissues which leads to nonspecifically targeted delivery of ^{125}I-GdNR agent.[16] Another possible reason is the enhanced blood flow in the inflammatory joint tissues which may also causes mildly elevated radioactivity.

The success in targeted delivery of GdNPs to inflammatory, an initial and common symptom of various types of pathogenesis, has been achieved for the first time by conjugating GdNPs with ICAM-1 monoclonal antibodies. Since the conjugates were tagged with ^{125}I radioisotopes, the *in vivo* performance of the newly designed agent as a function of time can be monitored using nuclear imaging, rendering a new and powerful method for convenient and quantitative assessment of novel nanoparticles as either agents for contrast enhancement or vehicles for drug delivery. A similar idea has been achieved before by using fluorescent tagging and optical imaging.[16] In comparison with fluorescent imaging, nuclear imaging could be a better choice for evaluation of nanoparticles considering the higher sensitivity, deeper imaging depth, whole-body imaging capability, and good quantification associated with nuclear imaging technology.

Delivery of radiolabeled GdNPs to the inflammatory tissues by specific targeting of monoclonal antibody-based biomarkers of inflammation could enable early detection and imaging of inflammation at molecular or cellular level by using both nuclear imaging and optical modalities such as PAI. Other than imaging, targeted delivery of GdNPs could also contribute to enhanced arthritis therapy in light of established benefits of gold treatment in inflammatory arthritis. In many previous studies, positive findings have been reported for clinical uses of gold compounds in the treatment of rheumatic diseases including psoriasis, juvenile arthritis, palindromic rheumatism, and discoid lupus erythematosus.[32−35] Other than arthritis, radioisotopes of gold have also found wide application in the regional treatment of different types of cancer.[36−39] All of these previous works using gold for cancer or arthritis therapy were based upon local injection, which inevitably limits the application and efficacy of gold-based treatment. Through the method reported in this work, gold particles with therapeutic potential for arthritis or cancer could be engineered for specific targeting of disease tissues and, hence, could be introduced systemically in the circulatory system.

In this work, the molecular targets chosen for specific delivery of GdNPs were ICAM-1, which was endothelial receptors overexpressed in newly formed vessels, such as vascular targets. Vascular targets are attractive because they appear very early in the disease process and allow easy access from the blood circulation. Moreover, for vascular targets, the particle sizes of the

contrast agent do not have to be smaller than the vessel pore cutoff size in order to achieve successful delivery.[40] Other than inflammation, it has been reported that ICAM-1 levels were elevated in several cancers including those associated with melanoma, ovarian, renal, prostate, leukemia, lung, and breast.[41,42] Due to the critical role of ICAM-1 in cancer generation and metastasis, the agent developed in this work could also prove useful for molecular imaging and early detection in a variety of cancers. Radiolabeled GdNR contrast agents, once uptaken by cancerous tissues, may also enable targeted therapy, including both radiotherapy facilitated by the radioisotope (*e.g.*, ^{131}I) and photothermal therapy as a result of the strong optical absorption of GdNPs. Therefore, by benefiting from both imaging and therapy, radiolabeling of GdNPs holds potential to be developed into a multifunctional medical platform for improved management of arthritis or cancer.

CONCLUSIONS

In this work, targeted delivery of GdNPs to the inflammatory tissues has been achieved by conjugating GdNPs with ICAM-1. Radiolabeling of the conjugates provides a highly efficient tool for early detection and imaging of inflammation at molecular level. The methodology developed here can be advanced to a level for clinical application by combining nuclear imaging and optical modalities. Furthermore, it is hoped that radiolabeled GdNP conjugates will become efficient therapeutic agents combining the power of radiation therapy and gold treatment for arthritis or cancer.

MATERIALS AND METHODS

Synthesis of the GdNRs. GdNRs were synthesized by a method modified from literature.[43,44] Briefly, a seed solution was prepared by reducing gold(III) chloride (25 μL, 0.05 M) in hexadecyltrimethyl ammonium bromide (4.7 mL, 0.1 M) by addition of freshly prepared sodium borohydride (0.3 mL, 0.01 M) under vigorous stirring. An aliquot of seed solution (0.24 mL) was added to the growth solution containing hexadecyltrimethyl ammonium bromide (100 mL, 0.1 M), gold(III) chloride (1.0 mL, 0.05 M), hydrochloric acid (2 mL, 1 M), 0.8 mL of ascorbic acid, and silver nitrate (1.2 mL, 0.01 M). The glass beaker was placed in a water bath maintained at 27 °C for 3 h to complete the synthesis. Then, 50 mL aliquots of the synthesized rods were centrifuged at 10 000 rpm for 1 h to obtain pellets of GdNRs at the bottom of the tube. The supernatant was decanted, and the pellet was redispersed into 5 mL of deionized water to get a concentration of 10^{13} rods/mL.

Covalent Conjugation of ICAM-1 Antibody on GdNRs. Covalent conjugation of ICAM-1 antibody was performed by bifunctional PEG linkers through well-established EDC/NHS (1-ethyl-3-[3-dimethylaminopropyl]carbodiimide hydrochloride and *N*-hydroxysulfosuccinimide) chemistry.[45] Briefly, 10 mg/mL of thiol-PEG-methyl (2 mM) and 2 mg/mL of thiol-PEG-carboxylic acid (0.4 mM) in water were first added to 1 mL of the CTAB-stabilized GdNRs (17 pM) and incubated at room temperature overnight to create PEG-stabilized GdNRs. The mixture was then washed by centrifugation to remove the excess PEG linkers. Five millimolar of EDC and SNHS (Sulfo-NHS) was added to the PEG-stabilized GdNR to activate the carboxylic group for 20 min. After activation, 50 μg of ICAM-1 antibody (0.3 nM) was injected into the activated PEG-GdNR mixture and incubated for 2 h to complete the reaction. The finished product was also washed by centrifugation. From final product, 20 μL of GdNR solution of each sample was dried on a copper grid coated with carbon film at room temperature. The dried conjugates of GdNR with ICAM-1 antibody were imaged in a JEOL 3011 high-resolution electron microscope.

Radiolabeling of GdNR Conjugates with Anti-ICAM-1. Covalent conjugates of ICAM-1 antibody with GdNRs were radiolabeled by mixing with [^{125}I] sodium iodide in deionized water at room temperature. In general, 0.2 mL of GdNRs with a concentration of 10^{13} rods/mL in deionized water was mixed with 0.1 mL of [^{125}I]NaI, roughly 300 μCi of radioactivity. The [^{125}I]-iodine-labeled GdNRs were then washed with deionized water by centrifugation. The pellets were redispersed into 200 μL of PBS for biological studies.

Enzyme-Linked Immunosorbent Assay of ICAM-1 Antibody. The ELISA plate was made in our laboratory. Briefly, 200 μL of 2 μg/mL rat recombinant ICAM-1 in ELISA coating buffer was added to each well of a 96-well plate and incubated for 12 h at room temperature. The coating solution was then aspirated out of the wells, and the wells were washed twice by ELISA washing buffer. Then, 300 μL of blocking buffer was added to each well and incubated for 4 h. After the blocking buffer was aspirated out the wells, the plate was ready for the screening experiment. In the screening experiment, 100 μL of radiolabeled PEGylated GdNR control and ICAM-1 antibody-conjugated GdNR solution was added to each corresponding well (30 μCi for each well) and incubated at room temperature for 2 h. Four wells were used for each GdNR sample in order to average the results. After 2 h, the solutions were removed from each well and the wells were washed by 300 μL of ELISA washing buffer twice. The well plate was dried (paper towel) and was then ready for radioactive analysis.

Radionuclide imaging was performed using the Gamma Imager (Biospace Lab, Paris). The planar imaging for ELISA experiments was performed with Gamma Imager detection area facing upward, and an ELISA plate was placed directly on the parallel-hole collimator 1.3/0.2/20 (hole diameter/septum thickness/height in mm). A 15 min duration image was acquired using the energy window 15−70 KeV, and the radioactivity of each well was then quantified using Gamma Vision+ software (version 3.0).

Gamma Imaging of Arthritic Rats *in Vivo*. All animal experiments were conducted in compliance with the Guidelines of the National Institutes of Health *Guide for the Care and Use of Laboratory Animals*. The protocol for these studies has been approved by the University of Michigan Committee on Use and Care of Animals. Female Lewis rats (125 g) were purchased from Charles River Laboratories (Wilmington, MA). To generate adjuvant-induced arthritis (AIA), the rats were injected subcutaneously into the base of the tail with lyophilized *Mycobacterium butyricum* (0.3 mL; Difco, Detroit, MI) suspended in mineral oil at 5 mg/mL. After day 20, a steep increase in clinical score of joint inflammation was observed, and the articular index (AI) scores of the affected rats were 3−4.

Before the imaging experiment, rats were anesthetized using isoflurane. An i.v. catheter was placed into lateral tail veins for systemic injection of the ^{125}I-labeled GdNR agents. For each animal, the injection of GdNRs (about 120 μCi) in 0.1 mL of PBS took 10 s. Then the catheters were rinsed with 0.2 mL of saline. Imaging was conducted on three groups, each containing five rats. Group A as a control was normal rats injected with targeting ^{125}I-ICAM-GdNR agent. Group B as another control was arthritic rats injected with nontargeting ^{125}I-GdNR agent. Group C was arthritic rats injected with targeting

^{125}I-ICAM-GdNR agent. Immediately after injection, each animal was imaged every hour with Gamma Imager for up to 4 h post-injection within the first day. The animals were reanesthetized and scanned at 24 h post-injection. Each image was acquired for 5 min on the anesthetized rat over the parallel-hole collimator 1.8/0.2/20 (hole diameter/septum thickness/height in mm) of the Gamma Imager. Animals were positioned ventral side down with the hind limbs placed in the middle of the filed of view of the imager; therefore, each image has a diameter of 8 cm covering the rear part of the rat body. With the images taken, radioactivity was then quantified by drawing regions of interest (ROI) using Gamma Vision+ software (version 3.0). For each animal, ROIs were drawn respectively around each ankle joint and the adjacent muscle area as the control. The ratios between the radioactivities from the inflammatory ankle joint and the non-inflammatory muscle were calculated based on radioactive counts.

Acknowledgment. This work was supported by National Institutes of Health Grant R01 AR055179. We thank Mariana Kaplan, M.D., for helpful discussion about the animal experiments.

REFERENCES AND NOTES

1. Minet, O.; Scheibe, P.; Beuthan, J.; Zabarylo, U.; Berlin, C. U.; Franklin, C. B. Correction of Motion Artefacts and Pseudo Colour Visualization of Multispectral Light Scattering Images for Optical Diagnosis of Rheumatoid Arthritis. *Laser Phys. Biophotonics* **2010**, *7547*, 75470B-1.
2. Visser, H. Early Diagnosis of Rheumatoid Arthritis. *Best Pract. Res., Clin. Rheumatol.* **2005**, *19*, 55–72.
3. Fan, P. T.; Leong, K. H. The Use of Biological Agents in the Treatment of Rheumatoid Arthritis. *Ann. Acad. Med. Singapore* **2007**, *36*, 128–134.
4. Choy, E. H.; Kingsley, G. H.; Panayi, G. S. Monoclonal Antibody Therapy in Rheumatoid Arthritis. *Br. J. Rheumatol.* **1998**, *37*, 484–490.
5. Malviya, G.; Conti, F.; Chianelli, M.; Scopinaro, F.; Dierckx, R. A.; Signore, A. Molecular Imaging of Rheumatoid Arthritis by Radiolabeled Monoclonal Antibodies: New Imaging Strategies To Guide Molecular Therapies. *Eur. J. Nucl. Med. Mol. Imaging* **2010**, *37*, 386–388.
6. Chianelli, M.; D'Alessandria, C.; Conti, F.; Priori, R.; Valensini, G.; Annovazzi, A.; Signore, A. New Radiopharmaceuticals for Imaging Rheumatoid Arthritis. *Q. J. Nucl. Med. Mol. Imaging* **2006**, *50*, 217–225.
7. Tong, L.; Wei, Q.; Wei, A.; Cheng, J. Gold Nanorods as Contrast Agents for Biological Imaging: Optical Properties, Surface Conjugation and Photothermal Effects. *Photochem. Photobiol.* **2009**, *85*, 21–32.
8. Oyeler, A. K.; Chen, P. C.; Huang, X.; El-sayed, H.; El-Sayed, M. A. Peptide-Conjugated Gold Nanorods for Nuclear Targeting. *Bioconjugate Chem.* **2007**, *18*, 1490–1497.
9. Niidome, T.; Akiyama, Y.; Shimoda, K.; Kawano, T.; Mori, T.; Katayam, Y.; Niidome, Y. *In Vivo* Monitoring of Intravenously Injected Gold Nanorods Using Near-Infrared Light. *Small* **2008**, *4*, 1001–1007.
10. Wang, Y.; Xie, X.; Wang, X.; Ku, G.; Bill, K. L.; O'Neal, D. P.; Stoica, G.; Wang, L. V. Photoacoustic Tomography of a Nanoshell Contrast Agent in the *In Vivo* Rat Brain. *Nano Lett.* **2004**, *4*, 1689–1692.
11. Chmberland, D. L.; Agarwal, A.; Kotov, N.; Fowlkes, J. B.; Carson, P. L.; Wang, X. D. Photoacoustic Tomography of Joint Aided by Etanercept-Conjugated Gold Nanoparticle Contrast Agent: An *Ex Vivo* Preliminary Rat Study. *Nanotechnology* **2008**, *19*, 095101.
12. Li, P. C.; Wei, C. W.; Liao, C. K.; Chen, C. D.; Pao, K. C.; Wang, C. R.; Wu, Y. N.; Shieh, D. B. Photoacoustic Imaging of Multiple Targets Using Gold Nanorods. *IEEE Trans. Ultrason. Ferroelectr. Freq. Control* **2007**, *8*, 1642–1647.
13. Song, K. H.; Kim, C.; Maslov, K.; Wang, L. V. Noninvasive *In Vivo* Spectroscopic Nanorod-Contrast Photoacoustic Mapping of Sentinel Lymph Nodes. *Eur. J. Radiol.* **2009**, *70*, 227–231.
14. Bhattacharya, R.; Mukherjee, P. Biological Properties of "Naked" Metal Nanoparticles. *Adv. Drug Delivery Rev.* **2008**, *60*, 1289–1306.
15. Fadeel, B.; Garcia-Bennett, A. E. Better Safe Than Sorry: Understanding the Toxicological Properties of Inorganic Nanoparticles Manufactured for Biomedical Applications. *Adv. Drug Delivery Rev.* **2010**, *62*, 362–374.
16. Kim, J.; Cao, L.; Shvartsman, D.; Silva, E. A.; Mooney, D. J. Targeted Delivery of Nanoparticles to Ischemic Muscle for Imaging and Therapeutic Angiogenesis. *Nano Lett.* **2011**, *11*, 694–700.
17. Liao, H.; Hafner, J. H. Gold Nanorod Bioconjugates. *Chem. Mater.* **2005**, *17*, 4636–4641.
18. Niidome, T.; Yamagata, M.; Okamoto, Y.; Akiyama, Y.; Takahashi, H.; Kawan, T.; Katayama, Y.; Niidome, Y. PEG-Modified Gold Nanorods with a Stealth Character for *In Vivo* Applications. *J. Controlled Release* **2006**, *114*, 343–347.
19. Takahashi, H.; Niidome, Y.; Niidome, T.; Kaneko, K.; Kawasaki, H.; Yamada, S. Modification of Gold Nanorods Using Phosphatidylcholine To Reduce Cytotoxicity. *Langmuir* **2006**, *22*, 2–5.
20. Eghtedari, M.; Liopo, A. V.; Copland, J. A.; Oraevsky, A. A.; Motamedi, M. Engineering of Hetero-Functional Gold Nanorods for the *In Vivo* Molecular Targeting of Breast Cancer Cells. *Nano Lett.* **2008**, *9*, 287–291.
21. Wang, C.; Chen, J.; Talavage, T.; Irudayaraj, J. Gold Nanorod/Fe_3O_4 Nanoparticle "Nano-Pearl-Necklaces" for Simultaneous Targeting, Dual-Mode Imaging, and Photothermal Ablation of Cancer Cells. *Angew. Chem., Int. Ed.* **2009**, *48*, 2759–2763.
22. Agarwal, A.; Shao, X.; Rajian, J. R.; Chamberland, D. L.; Kotov, N. A.; Wang, X. D. Dual Mode Imaging with Radiolabeled Gold Nanorods. *J. Biomed. Opt.* **2011**, *16*, 0513071–0513077.
23. Shao, X.; Agarwal, A.; Rajian, J. R.; Kotov, N. A.; Wang, X. D. Synthesis and Bioevaluation of ^{125}I-Labeled Gold Nanorods. *Nanotechnology* **2011**, *22*, 1351021–1351027.
24. Springer, T. A. Adhesion Receptors of The Immune System. *Nature* **1990**, *346*, 425–434.
25. Hopkinss, A. M.; Baird, A. W.; Nusrat, A. ICAM-1: Targeted Docking for Exogenous as Well as Endogenous Ligands. *Adv. Drug Delivery Rev.* **2004**, *56*, 763–778.
26. Dustin, M. L.; Rothlein, R.; Bhan, A. K.; Dinarello, C. A.; Springer, T. A. Induction by IL 1 and Interferon-Γ: Tissue Distribution, Biochemistry, and Function of a Natural Adherence Molecule (ICAM-1). *J. Immunol.* **1986**, *37*, 245–254.
27. Klimiuk, P. A.; Sierakowski, S.; Latosiewics, R.; Cylwik, J. P.; Skowronski, J.; Chwiecko, J. Soluble Adhesion Molecules (ICAM-1, VCAM-1 and E-Selectin) and Vascular Endothelial Growth Factor (VEGF) in Patients with Distinct Varients of Rheumatoid Synovitis. *Ann. Rheum. Dis.* **2002**, *61*, 804–809.
28. Kavanaugh, A. F.; Davis, L. S.; Nicholas, L. A.; Norris, S. H.; Rothlein, R; Scharschmidt, L. A.; Lipsky, P. Treatment of Refractory Rheumatoid Arthritis with a Monoclonal Antibody to Intercellular Adhesion Molecule 1. *Arthritis Rheum.* **1994**, *37*, 992–999.
29. Nakayamada, S.; Saito, K.; Fuji, i. K.; Yasuda, M.; Tamura, M.; Tanaka, Y. β 1 Integrin-Mediated Signaling Induces Intercellular Adgesion Molecule 1 and Fas on Rheumatoid Synovial Cells and Fas-Mediated Apoptosis. *Arthritis Rheum.* **2003**, *48*, 1239–1248.
30. Hiramitsu, T.; Yasuda, T.; Ito, H.; Shimizu, M.; Julovi, S. M.; Kakinuma, T.; Akiyosh, I. M.; Yoshida, M.; Nakamura, T. Intercellular Adhesion Molecule-1 Mediates the Inhibitory Effects of Hyaluronan on Interleukin-1β-Induced Matrix Metalloproteinase Production in Rheumatoid Synovial Fibroblasts *via* Down-Regulation of NF-Kb. *Rheumatology* **2006**, *45*, 824–832.
31. Storm, G.; Belliot, S. O.; Daemen, T.; Lasic, D. D. Surface Modification of Nanoparticles To Oppose Uptake by the Mononuclear Phagocyte System. *Adv. Drug Delivery Rev.* **1995**, *17*, 31–48.

32. Anandarajah, A. P.; Ritchlin, C. T. The Diagnosis and Treatment of Early Psoriatic Arthritis. *Nat. Rev. Rheumatol.* **2009**, *5*, 634–641.
33. Felson, D. T.; Anderson, J. J.; Meenan, R. F. The Comparative Efficacy and Toxicity of Second-Line Drugs in Rheumatoid Arthritis. Results of Two Metaanalyses. *Arthritis Rheum.* **1990**, *33*, 1449–1461.
34. Iii, C. S. Gold-Based Therapeutic Agents. *Chem. Rev.* **1990**, *99*, 2589–2600.
35. Tsai, C. Y.; Shiau, A. L.; Chen, S. Y.; Chen, Y. H.; Cheng, P. C.; Chang, M. Y. Amelioration of Collagen-Induced Arthritis in Rats by Nanogold. *Arthritis Rheum.* **2007**, *56*, 544–554.
36. Andrews, G. A.; Root, S. W.; Kerman, H. D.; Bigelow, R. R. Intracavitary Colloidal Radiogold in the Treatment of Effusions Caused by Malignant Neoplasms. *Ann. Surg.* **1953**, *137*, 375–381.
37. Wheeler, H. B.; Jaques, W. E.; Botsford, T. W. Experiences with the Use of Radioactive Colloidal Gold in The Treatment of Cancer. *Ann. Surg.* **1955**, *141*, 208–217.
38. Buchsbaum, H. J.; Keetel, W. C.; Latourette, H. B. The Use of Radioisotopes as Adjunct Therapy of Localized Ovarian Cancer. *Semin. Oncol.* **1975**, *2*, 247–251.
39. Rogoff, E. E.; Romano, R.; Hahn, E. W. The Prevention of Ehrlich Ascites Tumor Using Intraperitoneal Colloidal ^{198}Au. Dose *vs*. Size of Inoculums. *Radiology* **1975**, *114*, 225–226.
40. Schirner, M.; Menrad, A.; Stephens, A.; Frenzel, T.; Hauff, P.; Licha, K. Molecular Imaging of Tumor Angiogenesis. *Ann. N.Y. Acad. Sci.* **2004**, *101*, 67–75.
41. Rosette, C.; Roth, R. B.; Oeth, P.; Braun, A.; Kammerer, S.; Ekblom, J.; Denissenko, M. F. Role of ICAM1 in Invasion of Human Breast Cancer Cells. *Carcinogenesis* **2005**, *26*, 943–950.
42. Roland, C. L.; Harken, A. H.; Sarr, M. G.; Barnett, C. C. ICAM-1 Expression Determines Malignant Potential of Cancer. *Surgery* **2007**, *141*, 705–707.
43. Carb-Argibay, E.; Rodrguez-Gonzles, B.; Pacifico, J.; Pastoriza-Santos, I.; Perez-Juste, J.; Liz-Marzan, L. M. Chemical Sharpening of Gold Nanorods: The Rod-to-Octahedron Transition. *Angew. Chem., Int. Ed.* **2007**, *46*, 8983.
44. Perez-Juste, J.; Pastoriza-Santos, I.; Liz-Marzan, L. M.; Mulvaney, P. Gold Nanorods: Synthesis, Charaterization and Applications. *Coord. Chem. Rev.* **2005**, *249*, 1870–1901.
45. Hong, S.; Lee, D.; Zhang, H.; Zhang, J. Q.; Resvick, J. N.; Khademhosseini, A. Covalent Immobilization of P-Selectin Enhances Cell Rolling. *Langmuir* **2007**, *23*, 1226–1228.